Fisheries and Oceans Canada | Pêches et Océans Canada
Ecosystems and Oceans Science | Sciences des écosystèmes et des océans

Canadian Science Advisory Secretariat (CSAS)

Research Document 2016/090

Quebec Region

Spatial-temporal exposure of blue whale habitats to shipping noise in St. Lawrence system

Florian Aulanier[1,2], Yvan Simard[1,2], Nathalie Roy[1], Cédric Gervaise[3], and Marion Bandet[2]

[1] Fisheries and Oceans Canada
Maurice Lamontagne Institute,
850 route de la Mer,
Mont-Joli, Québec, Canada G5H-3Z4

[2] Marine Science Institute, University of Québec at Rimouski
310 Allée des Ursulines,
Rimouski, Québec, Canada G5L-3A1

[3] Université Grenoble-Alpes, Chaire Chorus,
Foundation of Grenoble Institute of Technology,
46, Avenue Felix Viallet, 38031
Grenoble cedex 1, France

September 2016

Canada

Foreword

This series documents the scientific basis for the evaluation of aquatic resources and ecosystems in Canada. As such, it addresses the issues of the day in the time frames required and the documents it contains are not intended as definitive statements on the subjects addressed but rather as progress reports on ongoing investigations.

Research documents are produced in the official language in which they are provided to the Secretariat.

Published by:

Fisheries and Oceans Canada
Canadian Science Advisory Secretariat
200 Kent Street
Ottawa ON K1A 0E6

http://www.dfo-mpo.gc.ca/csas-sccs/
csas-sccs@dfo-mpo.gc.ca

ISSN 1919-5044

Correct citation for this publication:

Aulanier, F., Simard, Y., Roy N., Gervaise, C., and Bandet, M. 2016. Spatial-temporal exposure of blue whale habitats to shipping noise in St. Lawrence system. DFO Can. Sci. Advis. Sec. Res. Doc. 2016/090. vi + 26 p.

TABLE OF CONTENTS

ABSTRACT

Blue whales frequenting the Estuary and Gulf of St. Lawrence are exposed to anthropogenic underwater noise from the main shipping route of Eastern Canada that connects the Great Lakes to the Atlantic, the St. Lawrence Seaway. This shipping underwater noise is concentrated in the low-frequency band used by baleen whales for their regular acoustic communications. The effects of this anthropogenic noise on the quality of this habitat of Northwest Atlantic blue whales, a population considered endangered under the Canadian *Species at Risk Act*, is a general concern. The first steps for assessing these effects include the establishment of the actual characteristics of this noise over time and space in the areas exploited by the whales throughout the annual cycle. This problem is addressed here by ground-truthed numerical simulations using information from *in situ* acoustic measurements, actual traffic, environmental conditions, and sound propagation modeling.

The cumulative distribution functions (cdf) of shipping noise radiated in blue whale call frequency band in the ~290 000 km^2 basin during typical summer and winter months were computed for 10 depth layers with a 1-km^2 resolution. This information was then used to map the risk of exceeding given noise thresholds or the likelihood of remaining under given noise levels, in an effort to identify at-risk and quiet areas. The role of the seaways and modulations by the three-dimensional (3D) basin shape are illustrated. The masking blue whale A- and D-calls by shipping noise was estimated with time budgets at representative locations in the Estuary and Gulf of St. Lawrence. Both calls are masked in the vicinity of shipping lanes, which fragment the communication space in several pieces. Compared to the prevailing conditions before the motorized shipping era, the masking by present shipping noise has much more affected the D-calls than the A-calls.

Exposition spatio-temporelle des habitats de la baleine bleue au bruit du trafic maritime dans le système Saint-Laurent

RÉSUMÉ

Les rorquals bleus fréquentant l'estuaire et le golfe du Saint-Laurent sont exposés aux bruits sous-marins d'origine anthropique de la principale route maritime de l'Est du Canada qui relie les Grands Lacs à l'Atlantique, la Voie Maritime du Saint-Laurent. Ce bruit de navigation sous-marin est concentré dans la bande des basses fréquences utilisée par les baleines à fanons dans leurs communications acoustiques régulières. Les effets de ce bruit anthropique sur la qualité de l'habitat des baleines bleues de l'Atlantique Nord-Ouest, une population considérée comme menacée selon la *Loi sur les espèces en péril* au Canada, est une préoccupation générale. Les premières étapes de l'évaluation des effets du bruit de navigation comprennent sa caractérisation dans le temps et l'espace, dans les zones exploitées par les baleines tout au long du cycle annuel. Ce problème est abordé ici par des simulations numériques validées, basées sur des mesures acoustiques *in situ*, le trafic maritime réel, les conditions environnementales et la modélisation de la propagation du son.

Les distributions cumulées (cdf) du bruit sous-marin de navigation dans la bande de fréquences des communications des rorquals bleus dans le bassin de ~ 330 000 km^2 ont été calculées pour 10 couches de profondeur avec une résolution de 1 km^2 pour des mois typiques d'été et d'hiver. Cette information a ensuite été utilisée pour cartographier le risque de dépasser des seuils de bruit donnés ou la chance de rester en-dessous de niveaux de bruit donnés, dans un effort d'identifier les zones à risque et les zones calmes du bassin. Le rôle des routes maritimes et les modulations par la forme tridimensionnelle (3D) du bassin sont illustrés. Les niveaux de masquage des vocalises A et B de la baleine bleue dû au bruit de navigation et leur probabilité d'occurrence ont été évalués à des points représentatifs dans l'estuaire et le golfe du Saint-Laurent. Les deux vocalises sont masquées dans les environs des voies maritimes, qui fragmentent les espaces de communication en plusieurs parties. Par comparaison aux conditions prévalent avant l'ère de la navigation à moteur, le masquage par le bruit de navigation a affecté beaucoup plus les vocalises D que les vocalises A.

TERMS AND ACRONYMS

AIS	automatic identification system
cdf	cumulative density function
CS	communication space, km^3 or km^2
CSQI	communication space quality index
DI	directivity index, dB
DT	detection threshold, dB
ECS_i	communication space effective i% of the time, km^3 or km^2
NL	noise level, dB re 1 µPa
NL_A	ambient noise level without shipping noise, dB re 1 µPa
NL_S	shipping noise level, dB re 1 µPa
PCS	potential communication space, km^3 or km^2
pdf	probability distribution function
PE	parabolic equation sound propagation model
RL	received level, dB re 1 µPa
SEL	sound exposure level over 24 h, dB re 1 μPa^2-s
SG	signal processing gain, dB
SL	source level, dB re 1 µPa @ 1 m
SNR	signal-to-noise ratio, dB
SPL	sound pressure level, dB re 1 µPa
T	A-call duration, s or dB re 1 s
TL	transmission loss, dB
W	frequency bandwidth, Hz or dB re 1 Hz

INTRODUCTION

The Northwest Atlantic blue whale (*Balaenoptera musculus*) population is estimated to have only a few hundred individuals (Sears and Calambokidis 2002) and is considered to be endangered under the *Species at Risk Act* of Canada since 2002 (Beauchamp et al. 2009). In addition to natural threats, the recovery strategy has identified several anthropogenic threats that may be affecting the small population. One of them, ranked as presenting a high-risk, is underwater anthropogenic noise in their environment, which has been considered as a potential source of habitat degradation that could trigger behavioral responses that may impact the population growth (Beauchamp et al. 2009). The transfer function from the threat to the effect on population may imply several pathways affecting the population dynamics (NRC 2005), including notably food access time-space restrictions, and masking vital communications and perception of their environment (Richardson et al. 1995, NRC 2003, Nowacek et al. 2007, Weilgart 2007). One of the prioritized actions of the recovery strategy to address this noise threat is to "*Identify/characterize noise sources and levels in different areas of the blue whale distribution range and assess the degree of exposure to the noise, particularly in the known areas of occurrence*" (Beauchamp et al. 2009). In the Northwest Atlantic- blue whale habitat in the Estuary and Gulf of St. Lawrence, the main source of underwater anthropogenic noise is regional and international shipping between the Atlantic and Great Lakes (Simard et al. 2014).

Blue whales frequenting the Estuary and Gulf of St. Lawrence are exposed to this underwater shipping noise that is concentrated in the low-frequency band used by baleen whales for their regular acoustic communications (e.g. Boyd et al. 2011). The blue whale vocal repertoire in North Atlantic and St. Lawrence is composed of three main call types: the 'A' and 'B' infrasounds between ~15-19 Hz and the audible low-frequency (~30-100 Hz) 'D' or 'arch' downsweep call (Mellinger and Clark 2003, Berchok et al. 2006). The infrasound source levels (SL) is estimated to ~190 dB re 1 µPa @ 1 m (McDonald et al. 2001, Širović et al. 2007), while the D-call SL is ~30 dB lower (Berchok et al. 2006). The frequency band between 15 Hz and 100 Hz should therefore be the main focus of first attempts to examine the masking effects of underwater noise on blue whale communication.

To evaluate this noise threat, the first steps are the establishment of the actual characteristics of this low-frequency noise, over time and space, in the areas exploited by the whales throughout the annual cycle. Since this latter information on whale distribution is still very fragmentary (Kingsley and Reeves 1998, Sears and Calambokidis 2002, Lawson and Gosselin 2009, Ramp and Sears 2012), especially outside summer and fall, properly addressing the threat in blue whale habitats of the Estuary and Gulf of St. Lawrence demands its evaluation over the entire spatial domain for representative periods of the annual cycle. This paper addresses this challenge by ground-truthed probabilistic shipping noise mapping, combining *in situ* measurements and numerical simulations fed by the actual AIS (Automatic Identification System) shipping traffic, estimated ship source levels (SL) of the fleet, environmental conditions from an operational hydrodynamic model and sound propagation modelling. Shipping noise cdfs are mapped for both the A-call and D-call frequency bands and used to identify at-risk and quiet areas. Then the communication space of blue whale calls and masking index are estimated for all encountered noise conditions, and used to assess the spatial and temporal distribution of the threat.

MATERIAL AND METHODS

To assess and map shipping noise in blue whale habitat for representative summer and winter months, monthly probability density functions (pdf) of sound pressure level (SPL) calculated with a temporal support (i.e. integration time unit) of 1s $(pdfSPL)_{1s}$ are computed on a grid of 1 km × 1 km horizontal resolution, and at 10 water depths from 10 m to 350 m for January and July. This is performed for conditions existing in 2013. Then, to evaluate the effects of this anthropogenic noise on masking blue whale calls and reducing their communication space relative to natural ambient noise, this shipping noise information is crossed with the knowledge on the blue whale acoustic communication at different locations (cf. Fig. 1).

SHIPPING SPL STATISTICS

To estimate monthly shipping noise statistics over the large basin and long periods of time, ocean acoustic simulations were performed every 30 min for the months of interest, representing a total of 1488 monthly statistical samples. Each sample represents a snapshot of the 3D shipping noise field corresponding to the instantaneous marine traffic, which can be used to generate one pdfSPL per voxel of the 1 km × 1 km node of the 10-layer 3D grid.

The simulation of such snapshots requires a large amount of contextual information determined by oceanographic, meteorological, geological and marine traffic conditions. First, the distribution of the acoustic sources includes every transiting ship at the instant *t* and their source level (SL) at the estimated acoustic frequency. Then, for each individual vessel, sound is propagated using ocean acoustic models to get the received acoustic levels at a given voxel of the volume, radiated by each ship in a neighborhood of 90 km. Finally, all the ship-specific received levels are added incoherently to get the total received level at the given voxel for the given frequency.

AIS PRE-PROCESSING

The ship traffic information comes from the AIS data recorded by the DFO-Coast Guard antenna network (cf. Simard et al. 2014). They were recorded over the whole Estuary and Gulf of St. Lawrence over the 2013 year time period (e.g. Fig. 2d, July 2013 mean daily traffic density for all ships). Ship GPS locations and ship characteristics (length, breadth, draught, speed, and category) were used to determine the acoustic source characteristics. The raw AIS data were subject to quality control and corrections before their use.

SHIP SOURCE LEVELS

Although ships are complex 3D acoustic sources (Ross 1976, Arveson and Vendittis 2000), in practice they are reduced to point-source equivalent (SL @ 1 m) for far-field measurements (ANSI 2009). Ship source horizontal locations have been set at the GPS position, and the effective source depths have been set using ship draught, when available, and ship length following (Gray and Greeley 1980).

Ships have been sorted in three length classes: smaller than 100 m, from 100 m to 250 m and longer than 250 m. SLs of the first class in 10 Hz to 100 Hz frequency band have been set to 150 dB re 1 µPa @ 1m according to Gervaise et al. (2012). For the other two classes, the SLs in the same band were obtained from those modeled from estimates based on measurements from an Acoustics Ship Signatures and Seaway observatory (AS^4) following ANSI/ASA-S12.64/Part 1 standard that was set up in St. Lawrence seaway in 2012-2013 (Fig. 3) (ANSI 2009, Simard et al. 2016a, Simard et al. 2016b).

ACOUSTIC PROPAGATION

The ocean acoustic propagation modelling was performed in the 10 Hz to 100-Hz frequency band with a split-step parabolic equation (PE) algorithm (Collins 1993, OALIB 2016). The PE algorithm design makes it particularly suited for efficient low-frequency highly range-dependent propagation (Jensen et al. 2011). However, even with an appropriate simulation model, the acoustic propagation still represents a substantial computational effort. To gain in efficiency, several approximations are made in the model and its parameterization. First, 3D propagation is approached by a 40 × 2D vertical sections around the source (i.e. 1 transect every 9 degrees), limited to a maximum range of 90 km. Second, sea-surface is considered to be ice-free, flat, and without sea-level variations. Elastic waves are not modelled in the ocean bottom (fluid equivalent bottom), and its structure has been defined as a 200-m thick sediment deposit lying on a semi-infinite bedrock. Sediment nature has been taken from Loring's and Nota's 1973 geological survey (Loring and Nota 1973) (Fig. 2b) and geo-acoustical properties have been approximated according to Jensen et al. (2011, table p. 39). Water-column acoustic properties have been computed from the temperature and salinity outputs of the Senneville and Lefaivre's ocean dynamic model (Senneville and Lefaivre 2015) and the Intergovernmental Oceanographic Commission standard TEOS-10 (McDougall and Barker 2011). Hourly sound-speed is obtained on a 5-km × 5-km grid and for 73 vertical layers covering the 540 m water column (e.g. Fig. 2c). For each simulated vertical section around a source, the mean water sound-speed profile of the nearest time sample is used. Sound absorption in water in the 10-100 Hz frequency band is very low, 10^{-3} dB km^{-1} at most, and is consequently neglected. Finally, bathymetric data (Fig. 2a) from the Canadian Hydrographic Service, interpolated on a 200-m mesh grid, is used for the bathymetry along the simulated vertical sections around a source.

To avoid strong boundaries effects the modeled zone has been extended ~100 km out of the Gulf at Cabot Strait (cf. Figs. 2b, c). In locations where no geological or temperature and salinity data were available, the environmental data have been extrapolated from the nearest informed neighbours.

With an average number of 128 ships simultaneously present in the Estuary and Gulf of St. Lawrence in July 2013, the number of propagation problems to solve is about 7 500 000 (i.e. 40 per ship). Considering that every PE acoustic run is taking a mean of 10 s on an Intel®Core(TM) i7-3930K CPU @ 3.20-3.60 GHz processor, it would have taken about 875 days to get shipping noise statistics for one month and a single frequency on a single-cored computer. The algorithm has therefore been implemented to run on 400 cores on the UQAR Mingan-cluster high performance computing facility, and it took a little more than two days to get the monthly shipping noise SPL simulation outputs and statistics.

ACOUSTIC DATA PROCESSING FOR GROUNDTRUTH VALIDATION

For validation purposes, shipping noise model outputs were compared to *in situ* measurements at the AS^4 observatory. However, *in situ* measurements not only contain shipping noise but also other anthropogenic noise, natural noise and pseudo-noise in low frequencies due to strumming, flow noise and mooring vibrations. AS^4 data contain mostly shipping and natural background noise, and tidally-recurrent low-frequency pseudo-noise. The relation between low-frequency pseudo-noise and tidal currents has been exploited to exclude the contaminated periods from the comparison. Tidal currents derived from local sea surface elevation showed a strong correlation (Pearson r^2 = 0.48) with 1-Hz to 100-Hz received levels. Therefore, for getting a less-contaminated acoustic subset for groundtruth comparisons, we filtered out acoustic samples corresponding to tidal currents exceeding the 40^{th} centile of the distribution. This second data subset is used for the comparison besides the non-filtered one.

HABITAT INSONIFICATION, RISK AND CHANCE

Two indicators of shipping noise exposure can be extracted from the simulated pdfSPL outputs to assess the relative habitat quality for blue whales in the studied region. The first one is the probability (or risk) to exceed a certain noise SPL threshold, which increases with degrading habitat quality, and allows highlighting the poor acoustic quality areas. The second is the probability (or chance) to remain below a given nose SPL value, which increases with habitat quality, and allows highlighting good acoustic quality areas. Risk is obtained by integrating the pdfSPL from the highest SPL down to a given threshold, and chance by integrating from the lowest SPL up to a given value.

To estimate shipping noise impact on behavior and internal ear injury, the following levels are considered. One often used such criterion for non-impulsive noise as an indicator for potentially triggering behavioral responses is a broadband SPL of 120 or 110 dB re 1µPa (Southall et al. 2007). This level criterion would correspond to 90 or 100 dB re 1 µPa in our one-third-octave centered at 16 Hz narrow-band SPL, from the approximate contribution of this narrow band to total shipping noise, whose energy is essentially concentrated below 400 Hz (Wenz 1962, Simard et al. 2010, Simard et al. 2016a). For low-frequency cetaceans, the sound injury criteria for non-impulsive noise are either a SPL of 230 dB re 1 $\mu Pa_{(peak)}$ or a events with a sound exposure level (SEL) of 215 dB re 1 μPa^2-s (Mlf-weighted) within a 24-h period (Southall et al. 2007).

COMMUNICATION SPACE

Communication space (CS) can be defined as the area over which an emitted call can be properly detected and interpreted by a receiving whale (Clark et al. 2009). Whale calls emitted with given source levels (SL) have their energy reduced by transmission losses (TL) while propagating through the ocean before reaching a receiver with a lower received level (RL). For a communication to be successful, the receiving whale needs to discriminate and interpret this signal of primal interest amongst a crowd of other sounds that are qualified as noise. This process involves many factors that can be separated into receiver-independent and receiver-dependent factors.

In the first factor type, we have the call RL, the noise level (NL), and more particularly how these two levels compare to each other, i.e. the signal-to-noise ratio (SNR, in dB):

$$SNR = RL - NL[dB], with\ RL = SL - TL\ [dB\ re\ 1\ \mu Pa]$$

The RL dependence on SL and TL links it to the call characteristics and the 3D location in the ocean. NL is made of two components: shipping noise level (NL_S), and ancient ambient noise level (NL_A) such as:

$$NL = 10 \times log_{10}(10^{(NL_S/10)} + 10^{(NL_A/10)})\ [dB\ re\ 1\ \mu Pa]$$

In the receiver-dependent factors, we have the whale individual ability to discriminate sounds from their directions-of-arrival, frequency contents and time structures, including contextual information. Most of this information is essentially unknown for blue whales but some bounds can be estimated from analogy with sonar systems. Considering an A-call duration (T) of 13.8 s and a bandwidth (W) of ~0.8 Hz over most of the call (Berchok et al. 2006), the estimated blue whale A-call signal processing gain (SG = $10 \times \log_{10}(TW)$, (Clark et al. 2009)) is ~10 dB. Likewise, D-call SG would be ~20 dB (with a T of ~2 s and a W of ~50 Hz, (Berchok et al. 2006)). The gain brought by directivity (DI) is unknown and considered to be 0 dB to remain conservative (Clark et al. 2009). Lastly, the receiver detection threshold (DT) required to get a 50% detection success is considered to be ~10 dB (Kastelein et al. 2007). Assuming 50% of

detection is the minimum performance necessary to allow a successful communication (Clark et al. 2009), then the communication is effective when:

$$SNR \geq DT - DI - SG \cong \begin{cases} 0\ dB, for\ A\ calls \\ -10\ dB, for\ D\ calls \end{cases}$$

Therefore, hereafter we consider a SNR of 0 dB as a first approximation to define an "*effective communication*".

EFFECTIVE COMMUNICATION SPACE AND ITS QUALITY INDEX

The CS can be affected by maskers such as shipping noise. Therefore to assess the effect of shipping noise we need to define:

a) a reference CS, the potential CS (PCS), corresponding to the ancient ambient noise;

b) a CS quality index, CSQI, equivalent to the probability that a communication is effective at a location in the reference CS, which tells the proportion of time, *i*, the communication is locally possible;

c) an effective CS (ECS), corresponding to locations where CSQI exceeds a given threshold, *i*, (ECS_i).

Examples of PCS and ECS_{99} are mapped in Figs. 10c and 10d respectively for an emission scenario at the point of interest 1 of Fig. 1. The relation of ECS_i as function of *i* can be seen in Fig. 12a. These spaces are actually volumes but we focus here on their most-relevant depth slice, and assess the areas in km^2. Since absolute ECS_i areas highly depend on the topography around the points of interest, they are also normalized by the areas in the ancient ambient noise conditions (Figs. 12b and 13b).

SENDER ECS_I AND CSQI EVALUATION AT 6 POINTS OF INTERESTS IN THE ST. LAWRENCE GULF

An evaluation of the sender[1] communication space quality is made at 6 points of interest (Fig 1) in the traffic and environmental conditions of July 2013. As first approximation, blue whales are considered to be omnidirectional low-frequency point sources emitting at 15-m depths (Oleson et al. 2007) with a SL of 190 dB re 1 µPa @ 1 m in the 16-Hz centered one-third-octave band for A and B calls (McDonald et al. 2001, Širović et al. 2007), and a SL of 160 dB re 1 µPa @ 1 m for D calls in the 63-Hz centered one-third octave band (Berchok et al. 2006). As receivers, blue whales are assumed to follow krill concentrations and spend most of their time in the first 150 m of the water column (Simard et al. 2003, Doniol-Valcroze et al. 2012, Lavoie et al. 2015). To compute the CSQI, call RLs computed for receiving whales at 50-m depth, were compared to shipping noise percentiles of July 2013, and ancient ambient noise levels are taken from Gervaise et al. (2012)'s estimate for the Saguenay-St. Lawrence Marine Park. At a given location in the CS, the CSQI is therefore determined as the shipping-noise percentile value at which the SNR is 0.

[1] In this paper we only consider the communication space centered on the source. The one centered on the receiver is different and can be estimated using the same approach.

RESULTS

SHIPPING NOISE MODEL VALIDATION USING IN SITU MEASUREMENTS

Simulated shipping noise SPLs show good agreement with measurements, both for the mean SPL and the pdfSPL at the different frequencies (Fig. 4). The fit with all-measurements pdfSPL is better at 40-Hz or 63-Hz modeled frequencies of than at the 20-Hz and 16-Hz lower frequencies, where the pdfSPL is shifted towards higher SPL values that are not found in simulated SPLs. It reveals the presence of a second mode clearly established at the 62-m depth and 20-Hz frequency. These high SPL values in measurements are in all likelihood due to current-induced flow noise around the hydrophone, mooring vibrations and strumming, which prominently affect the low frequencies. After removing the 60% of the samples where the estimated tidal currents were the strongest, much better fits of the simulated and the measured SPLs at the 16-Hz and 20-Hz frequencies are observed at all depths. The pdfSPL for the 40-Hz and 60-Hz higher frequencies remained unchanged. The difference in the cumulative distribution function (cdf) of the simulated and the pseudo-noise filtered *in situ* SPL for the different frequencies and depths varies from 0.0 ± 2.8% to 2.7 ± 5.7% standard deviation (S.D.) (Table 1). With the raw *in situ* SPL, it was 0.0 ± 2.8% to 5.6 ±12.1 % (S.D.). These difference estimates represent the errors in the risk estimates mapped in the next sections.

SHIPPING NOISE STATISTICS

The probability of shipping noise in the study region was mapped for the 5^{th}, 25^{th}, 50^{th}, 75^{th}, 95^{th}, and 99^{th} percentiles for the 16-Hz and 63-Hz one-third-octave band at two different depths, 25 m and 75 m, that blue whales exploit for feeding over the diel cycle (Figs. 5, 6). These maps show that horizontal extent of shipping noise exposure is greatly related with the distance to traffic lanes and traffic density (Fig. 2d). In low traffic densities ($<5^{th}$ percentile) the effect is perceptible above background noise only in the deep Laurentian Channel where the main shipping route is located. In high traffic conditions ($> 95^{th}$ percentiles), the shipping noise effect has spread over the entire studied areas, except in shallow waters and under very low traffic densities. The effects are stronger at the 63-Hz one-third-octave band (Fig. 6), because of the higher ship SL at this frequency (Fig. 3, (Simard et al. 2016a)) and weaker transmission losses.

The effect of bathymetry (Fig. 2a) on shipping noise SPL modulations is noticeable in various areas. Spatial variations due to water column properties can also be observed, but they tend to be smaller.

A frequency × depth synopsis of shipping noise SPL and ambient noise received at point of interest 3 (Fig. 1) shows that shipping noise excess relative to mean ambient noise level (ANL) ranges from 0 to 70 dB. The main mode varies with frequency and depth from ~10 dB for the 16-Hz one-third-octave band at 10 m to ~30 dB for the 40-Hz and 63-Hz one-third-octave bands over the entire water column. Shipping noise SPL tends to be 20 to 30 dB louder at these latter higher frequencies compared to the lower ones (see also Figs. 5 and 6). At the 16-Hz and 20-Hz frequencies, shipping noise tends to be 5 to 10 dB weaker closer to the surface than further down in the water column. Simulated seasonal effects related to changes in vertical structure of water masses were rather small (< ~±3 dB) at points of interest (Fig. 7), illustrating the weak sensitivity of low-frequency sound propagation to water column sound speed profile. However, seasonal effects are specific to local ocean dynamics and can be different at other locations, especially in shallow waters.

CHANCE AND RISK MAPS

Risk, or chance, to exceed or be lower than a given shipping noise SPL threshold criterion can be computed from the pdfSPL illustrated by a few percentiles on Figs. 5 and 6.

The risk, or chance, to exceed or be under 90-dB or 100-dB one-third-octave narrow-band thresholds varies with location, depth, frequency and season (e.g. Figs. 8, 9, for 16-Hz one-third-octave band at 25-m and 75-m depths). Close to point of interest 3, the risk that shipping noise 16-Hz one-third-octave SPL exceeds 90 dB re 1 µPa reaches 20 to 30% in a 20-km wide corridor around the main shipping route (Fig. 8a, b). This means that, in July 2013, shipping noise SPL received in this corridor has been above 90 dB re 1 µPa for about one third of the time at this depth. The risk to exceed 100 dB re 1 µPa however hardly reaches 5% within a 3-km wide corridor around both inward and outward lanes of the shipping route (Fig. 8c,d). This means that intense SPL can be heard from time to time, most likely when ships are passing close by.

In contrast, quiet areas where shipping noise never exceeds 90 dB re 1 µPa more than 5% of July 2013 are all areas away from the main seaway at 25-m depth (Fig. 9a) but this area is reduced by at least half at the deeper 75-m depth (Fig. 9b). Locations where shipping noise remains under 100 dB re 1 µPa at least 99% of the time in July 2013 are those a few kilometeres away from the shipping routes (Fig. 9c, d). In other words, there is a 99% chance that these areas remain quieter than 100 dB re 1µPa in July.

COMMUNICATION SPACE QUALITY INDEX

As described in the material and methods section, shipping noise statistics are used to evaluate blue whale CSQI at 6 points of interest (see Fig. 1). Fig. 10a illustrates the received levels at 50-m depth within a 200-km radius around point 1, when a 15-m deep blue whale emits a 190-dB re 1 µPa @ 1 m 16-Hz one-third-octave band A-call. The corresponding 50-m depth PCS considering an ancient ambient noise level of 65 dB re 1 µPa in this same band is mapped on Fig. 10c, and corresponds to an area of approximately 10 000 km^2. Fig. 12 shows the ECS_i, the amount of this pristine condition CS exceeding a given CSQI threshold for different values of CSQI. We can observe that only one third of the PCS shows a CSQI of at least 99% (Fig. 12b), corresponding to areas where the communication is nearly always possible (i.e. at least 99% of the time). Lower CSQI locations clearly reflect shipping lanes footprints. CS with a CSQI exceeding 80% (ECS_{80}) and 90% (ECS_{90}) are shown in Figs. 10e, f, and 12a, b and show that low CSQI areas are located preferentially close to the shipping lanes and far from the sender. Similar effects are observed at other receiving depths.

The A-call transmission is repeated in the neighborhood of point 2 (Fig. 11a), where the pristine CS at 50-m depth is estimated to ~ 30,000 km^2 (Figs. 11c, 12a). CS with a CSQI of at least 99% (ECS_{99}) – where communication is still possible when shipping noise locally reaches its 99th percentile (Fig. 11b) – represent here ~43 % of the PCS (Fig. 11d and 12b). Again, strongest CSQI reductions are observed close to shipping lanes or far from the sender (Figs. 11d, 12b). CS corresponding to CSQIs of at least 80% (ECS_{80}) and 90% (ECS_{90}) are shown in Figs. 11e, f, 12a, b.

In the absence of shipping noise, the absolute PCS depends strongly on location (Fig. 12a). Masking effects are related to the proximity to dense traffic area and low-frequencies propagation characteristics around the location of emission. For instance, unlike points 1 and 2, in the Esquiman Channel (point of interest 6, Fig. 1) no reduction of the CSQI is observed during 75% of the month of July (Fig. 12). Then, for the loudest 10% of July shipping noise (i.e. 90th shipping noise percentile), the ECS_{90} still represents 90% of the PCS. Finally, during the

noisiest 1% of the time, the ECS_{99} is reduced to a maximum of 70% of the original shipping-noise free value (i.e. PCS).

Blue whale D-calls, transmitted in the 63-Hz one-third-octave band with a source level of 160-dB re 1 µPa @ 1 m, are also affected by shipping noise. Their PCS are only slightly smaller than A-call ones under ancient-ambient-noise condition. They are, however, much more affected by shipping noise than the 16-Hz A-call (Fig. 13). CS with a CSQI of at least 33% (ECS_{33}) only represent at most 20% of the PCS in the surrounding of points of interest 1, 2, 3, and 5 (Figs. 1,13b). This means that D-call ECS_{66} are reduced by at least 80% during the two-thirds of the month of July in comparison to PCS. Again, the situation is less critical in the vicinity of points 4 and 6 where the shipping traffic is sparser. 80% of the pristine CS has a CSQI of at least 60% (Fig. 13 b), which means that in these areas communication is interrupted at most 40% of the time, i.e. when a ship is passing.

DISCUSSION

An assessment of shipping noise in blue whale habitats in the Estuary and Gulf of St. Lawrence has been done. The advantage of having estimated the entire distribution of shipping noise SPL during representative months of the annual cycle instead of usual single annual or monthly mean estimates allows to better investigate in time and space the exposure risk to critical high levels, as well as masking effects (cf. Gervaise et al. 2015). Such shipping noise pdf statistics are required to evidence the continuum of varying conditions over time that allows identifying quiet areas and areas at-risk, and the relative probability of exposure.

Underwater noise is fundamentally structured in time and the 3D space. Measurements series at one 3D location cannot be automatically generalized to the whole volume of a large basin. To do this, acoustic modelling is needed. Proper simulation modeling however requires careful configuration and implementation to be able to reproduce *in situ* observations with accuracy and precision. The relatively good reproduction of the observed SPL variability at 3 depths of the water column at the AS^4 seaway observatory make us confident that the simulated results are reproducing the observed noise characteristics, with its central statistics and variability, with a reasonably low error level. This general good agreement between simulations and measurements has been made possible thanks to the use of a St. Lawrence's-fleet-specific ship-SL model based on AS^4 seaway observatory (Simard et al. 2016b, Simard et al. 2016a), the output of a ground-truthed hydrodynamic model (Senneville and Lefaivre 2015) and the choice of appropriate acoustic propagation model (Jensen et al. 2011, Farcas et al. 2016). Of course, the modelling configuration and approach can be perfected as the required input information is improved, but we are confident that the first order effects were realistically taken into account. For example, risk maps of Fig. 8 show that even less-frequented secondary shipping routes present a risk to exceed 100-dB re 1 µPa SPL in the blue whale A-call band, even if the probability remains low in comparison to main seaways.

The shipping noise quantile maps in the blue whale call band showed higher values on or very close to the shipping route, in agreement with other spatial mapping studies in the Canadian west coast (Erbe et al. 2012, Erbe et al. 2014). In the present study, the use of a PE acoustic model propagation parameterized with range-dependent bathymetry, instead of geometrical spreading laws plus frequency dependent absorption and shallow water cut-off frequency, allows us to show that acoustic energy tends to be first constrained within the Laurentian Channel before spreading over with increasing traffic density. This strong bathymetric effect is clearly seen in Fig. 5d, for instance on the margin of the Magdalen shelf and southern slope of the Laurentian Channel. In other cases, increasing depths in the Laurentian Channel affected lower SPL quantiles values, as seen south of the Anticosti Island (Fig. 6a) at a location where

the bathymetry goes down to 450 m (Fig. 2a). The same effect is observed at the northern entrance of Cabot Strait (Fig. 5c) where the bathymetry deepens to more than 500 m (Fig. 2a).

Footprints of water-column properties are more difficult to observe since they vary independently from ship passages and were averaged before performing the propagation along the 2D vertical transect. However, regions with large water property gradients seems to concord with noise level variations. For example, close to the northern coast of the Strait of Belle-Ile, near Blanc-Sablon, is an area regularly experiencing locally warmer temperatures (Fig. 2c), and showing more intense shipping noise SPL quantile (Fig. 5f). Horizontal distribution variations in the Cabot Strait (Fig. 5d) might also be explained partially by the recurrent presence of strong gradients (Fig. 2c). However, considering the complexity of bathymetry and ocean dynamics, it has to be acknowledged that a better understanding of the horizontal structure could be obtained by full 3D propagation modelling (Badiey et al. 2005, Sturm 2005), an approach which unfortunately involves prohibiting computational costs. Another limitation of the model can be seen at about 90 km off the main seaways (Fig. 6d) where the propagation modelling from the source attains it maximum range. Although, shipping noise SPL is low at this range, this 90-km limit should be removed in future simulations since it might have an effect on estimated whale communication space. Thick ice covers with occasional deep keels as in multi-year Arctic ice is also known to affect acoustic propagation. This has not been considered here since the ice in the Estuary and Gulf of St. Lawrence is much thinner and sparser. Besides, the effect of this ice roughness requires the development of dedicated modelling that is beyond the scope of the present study.

Variations of pdfSPL with frequency (Fig. 7) can be partly explained by ship SL spectral pattern (Fig. 3), for a proportion of 5 dB of the whole 20-dB variation. The rest of the variation with frequency could result from acoustic propagation characteristics where lower frequencies are penetrating deeper in bottom sediment layers and are more attenuated in shallow waters.

Measurement and simulation results show that none of the non-impulse sound injury criteria are likely to be reached in the study area, unless a whale follows a ship at 100-m distance for 24 hours in a row. The risk maps (Fig. 8) however indicate that behavioral effect could likely be triggered within a 20-km range envelope around the main seaways during 30 % of the time, and within about 1-km of secondary routes for 5% to 10% of the time. Indeed, the largest part of the St. Lawrence Gulf remains a relatively quiet area as indicated on the chance maps (Fig. 9). In particular, the fact that the main shipping route is located in the middle of the Laurentian Channel tends to mitigate the possible disturbance on the slopes were the currents concentrate their food (Lavoie et al. 2000, Simard 2009, Lavoie et al. 2015).

The effects of shipping noise on communication can be examined through the CSQI. Simulations clearly showed that the size of the PCS is strongly dependent on locations in the basin, whose propagation characteristics are not uniform but variable in space. For the 6 points of interest examined, the PCS absolute area can vary by a factor of at least 6 for both the A-call infrasound and the audible D-call. Maximizing communication space in a non-homogeneous basin is therefore a location problem, even under conditions of no shipping noise. The effect of shipping noise on CS dramatically differs for the 2 call types. Under natural ambient noise conditions, the PCS area can reach 60 thousand km^2 for both calls. For the 4 points of interest where shipping is not negligible (i.e. 1,2,3, and 5), the D-call ECS_i decreases exponentially for CSQIs up to 20% (Figs. 13 and 2d), which shows that the PCS is affected by the lowest 20% of shipping noise. For the A-call, the ECS_i only slowly decreases in the first 80^{th} to 90^{th} shipping noise centiles (i.e. CSQI) before plunging in the highest decile for all 6 points of interest to reach 30% of the PCS (Fig. 12). It appears therefore that in the study area, the shipping noise imprint on blue whale communication compared to ancient pristine conditions was much more severe for the D-call than for the A-call.

Simulations show that communication range can extend to more than 200 km, in absence of terrestrial boundaries and bathymetry restrictions such as the ~40-km wide Laurentian Channel in Lower St. Lawrence Estuary (Fig. 10c). The CS is more affected by the interactions with bathymetry and shipping noise than by the attenuation due to propagation range. Indeed, the greatest reduction is obtained when a ship is passing close to the caller and local shipping noise reaches a maximum. Then 30 to 65% of the area can be affected in the case of A-calls (Fig. 12b) and 100% in the case of D-calls (Fig. 13b). Present work sheds new light on how CS are spatially affected. Simulations showed that shipping lanes can cut a CS into several pieces rather that only reducing it (e.g. Figs. 10d, 11d). This means that there exists a probability that communication with remote individuals is maintained while it has been masked for closer animals.

To assess shipping noise impact ECS_i and CSQI were preferred to the masking index and its percentiles as defined in Clark et al. (2009). The main difference between these metrics lies in the way these two indices treat the CS spatially. The masking index looks at the masking of the CS as a whole, whereas the CSQI considers the masking of every pieces of the CS individually. Using the CSQI allows us to gain an insight on the sender CS at a given location showing which part is often masked. This is of practical interest for habitat quality assessment. However, the two indices show similar relative trends when CS pieces are considered together.

With a better knowledge on blue whale habitat spatial distribution and time frequentation (e.g. maps of probability of blue whale presence), CQSI could be used to visualize areas and proportion of time where shipping noise effectively mask blue whale communications. Converting this pressure to estimate the effects of chronic communication masking on blue whale population fecundity or rate of survival is a step further. Unfortunately, the knowledge gaps to bridge before reaching the needed levels to feed such complex models (e.g. PCAD, NRC 2005) with reasonable certainty for blue whales still represents a hardly achievable challenge.

CONCLUSION

The probability of low-frequency shipping noise – in depth layers representative of those exploited day and night by blue whales feeding on krill – spreads from the shipping lanes with ranges increasing with traffic, and is modulated with bathymetry principally. The shipping noise in the D-call frequency band tends to be 20-30 dB higher than that of the A-call infrasonic band, likely in response to bottom propagation characteristics and partly due to higher radiating noise by ships at these frequencies. The noise excess due to shipping, relatively to natural ambient level, can reach 70 dB, with modal values varying with depth and frequency from 10 to 30 dB, and 5 to 10 dB weaker values in the infrasonic band near the surface compared to deeper depths. Modulations by summer/winter seasonal change in water mass vertical profile were weak for the 10-100 m depth layers explored.

The risk that shipping noise levels exceed injury criteria for low-frequency marine mammals is considered to be nil. However, the risk to exceed low SPLs inducing behavioral responses might exist up to 30% of the time at proximity to the shipping lanes, with ranges varying from few km up to about 20 km. This risk is more likely to exist 5% of the time within about 5 km around the main seaway in the Laurentian Channel for a 10-dB higher SPL noise criterion. Inversely, a large portion of the entire study area has a low probability of receiving shipping noise levels exceeding thresholds likely to trigger behavioral reactions. The location of the main seaway in the middle of the ~20-50 km wide Laurentian Channel reduces the possibility of high shipping noise on the channel slopes where blue whale food is known to aggregate.

Simulated communications in 6 locations representative of diverse conditions showed that the CS is large and of the same order of magnitude for both A-calls and D-calls under natural ambient noise conditions. For A-call, at 50-m depth, 85% of the PCS is masked less than 40% of the time. However, PCS areas that are never affected by masking can shrink up to 66% into the Laurentian Channel. The PCS area of the 30-dB weaker D-call is reduced by 90% for about 90% of the time in the vicinity of the Laurentian Channel. In other locations with low shipping traffic, D-call communication probability area remains unaffected 70% of the time, but it vanishes almost entirely 10% of the time when traffic is present. Traffic lanes not only reduce communication spaces but they can cut them into several pieces.

ACKNOWLEDGEMENTS

Funding support from Fisheries and Oceans Canada, Natural Sciences and Engineering Research Council of Canada Discovery grant to Y. Simard, and the Chair Chorus of the Grenoble Institute of Technology Foundation to C. Gervaise are gratefully acknowledged. This work benefited from UQAR “Mingan” cluster computing facility and in particular James Caveen for precious help in the implementation. We thank Denis Lefaivre and Simon Senneville for sharing the outputs of their ocean dynamic model and Alain D’Astous for his help in temperature salinity data processing.

REFERENCES

ANSI. 2009. Quantities and procedures for description and measurement of underwater sound from ships – Part 1: General Requirements. *In* Accredited Standards Committee S12, Noise. Acoust. Soc. Am. Standards Secretariat, N.Y. p. 21 p.

Arveson, P.T., and Vendittis, D.J. 2000. Radiated noise characteristics of a modern cargo ship. J. Acoust. Soc. Am. 107(1): 118-129.

Badiey, M., Katsnelson, B.G., Lynch, J.F., Pereselkov, S., and Siegmann, W.L. 2005. Measurement and modeling of three-dimensional sound intensity variations due to shallow-water internal waves. J. Acoust. Soc. Am. 117(2): 613-625.

Beauchamp, J., Bouchard, H., de Margerie, P., Otis, N., and Savaria, J.-Y. 2009. Recovery strategy for the blue whale (*Balaenoptera musculus*), Northwest Atlantic population, in Canada. Species at Risk Act Recovery Strategy Series Fisheries and Oceans Canada, Ottawa.

Berchok, C.L., Bradley, D.L., and Gabrielson, T.B. 2006. St. Lawrence blue whale vocalizations revisited: Characterization of calls detected from 1998 to 2001. J. Acoust. Soc. Am. 120(4): 2340-2354.

Boyd, I.L., Frisk, G., Urban, E., Tyack, P., Ausubel, J., Seeyave, S., Cato, D., Southall, B., Weise, M., Andrew, R., Akamatsu, T., Dekeling, R., Erbe, C., Farmer, D., Gentry, R., Gross, T., Hawkins, A., Li, F.H., Metcalf, K., Miller, J.H., Moretti, D., Rodrigo, C., and Shinke, T. 2011. An international quiet ocean experiment. Oceanogr. 24: 174-181.

Clark, C., Ellison, W.T., Southall, B.L., Hatch, L., Van Parijs, S., Frankel, A.S., and Ponirakis, D. 2009. Acoustic masking in marine ecosystems: intuitions, analysis, and implication. Mar. Ecol. Prog. Ser. 395: 201-222.

Collins, M.D. 1993. A split-step Padé solution for the parabolic equation method. J. Acoust. Soc. Am. 94(4): 1736-1742.

Doniol-Valcroze, T., Lesage, V., Giard, J., and Michaud, R. 2012. Challenges in marine mammal habitat modelling: evidence of multiple foraging habitats from the identification of feeding events in blue whales. Endang. Sp. Res. 17(3): 255-268.

Erbe, C., MacGillivray, A., and Williams, R. 2012. Mapping cumulative noise from shipping to inform marine spatial planning. J. Acoust. Soc. Am. 132(5): EL423-EL428.

Erbe, C., Williams, R., Sandilands, D., and Ashe, E. 2014. Identifying modeled ship noise hotspots for marine mammals of Canada's Pacific region. PLOS ONE 9(3): e89820.

Farcas, A., Thompson, P.M., and Merchant, N.D. 2016. Underwater noise modelling for environmental impact assessment. Environmental Impact Assessment Review 57: 114-122.

Gervaise, C., Simard, Y., Roy, N., Kinda, B., and Menard, N. 2012. Shipping noise in whale habitat: characteristics, sources, budget, and impact on belugas in Saguenay - St. Lawrence Marine Park hub. J. Acoust. Soc. Am. 132: 76-89.

Gervaise, C., Aulanier, F., Simard, Y., and Roy, N. 2015. Mapping probability of shipping sound exposure level. J. Acoust. Soc. Am. 137(6): EL429-EL435.

Gray, L.M., and Greeley, D.S. 1980. Source level model for propeller blade rate radiation for the world's merchant fleet. J. Acoust. Soc. Am. 67(2): 516-522.

Jensen, F.B., Kuperman, W.A., Porter, M.B., and Schmidt, H. 2011. Computational ocean acoustics. Springer.

Kastelein, R.A., de Hann, D., and Verboom, W.C. 2007. The influence of signal parameters on the sound source localization ability of a harbor porpoise (*Phocoena phocoena*). J. Acoust. Soc. Am. 122: 1238–1248.

Kingsley, M., and Reeves, R.R. 1998. Aerial surveys of cetaceans in the Gulf of St. Lawrence in 1995 and 1996. Can. J. Zool. 76(8): 1529-550.

Lavoie, D., Simard, Y., and Saucier, F.J. 2000. Aggregation and dispersion of krill at channel heads and shelf edges: The dynamics in the Saguenay - St. Lawrence Marine Park. Can. J. Fish. Aquat. Sci. 57(9): 1853-1869.

Lavoie, D., Chassé, J., Simard, Y., Lambert, N., Galbraith, P.S., Roy, N., and Brickman, D. 2015. Large-Scale Atmospheric and Oceanic Control on Krill Transport into the St. Lawrence Estuary Evidenced with Three-Dimensional Numerical Modelling. Atmos. Ocean: 1-27.

Lawson, J.W., and Gosselin, J.F. 2009. Distribution and preliminary abundance estimates for cetaceans seen during Canada's marine megafauna survey - A component of the 2007 TNASS. DFO Can. Sci. Adv. Sec. Res. Doc. 2009/031. vi + 28

Loring, D.H., and Nota, D.J.G. 1973. Morphology and sediments of the Gulf of St. Lawrence. Bull. Fish. Res. Bd. Can. 182: 147 p. + 147 charts.

McDonald, M.A., Calambokidis, J., Teranishi, A.M., and Hildebrand, J.A. 2001. The acoustic calls of blue whales off California with gender data. J. Acoust. Soc. Am. 109(4): 1728-1735.

McDougall, T.J., and Barker, P.M. 2011. Getting started with TEOS-10 and the Gibbs Seawater (GSW) oceanographic toolbox. SCOR/IAPSO WG127.

Mellinger, D.K., and Clark, C.W. 2003. Blue whale (*Balaenoptera musculus*) sounds from the North Atlantic. J. Acoust. Soc. Am. 114(2): 1108-1119.

Nowacek, D.P., Thorne, L.H., Johnston, D.W., and Tyack, P.L. 2007. Responses of cetaceans to anthropogenic noise. Mamm. Rev. 37(2): 81-115.

NRC. 2003. Ocean noise and marine mammals. National Academy Press, Washington D.C.

NRC. 2005. Marine mammal populations and ocean noise: Determining when noise causes biologically significant effects. National Academy Press, Washington D.C.

OALIB. 2016. Ocean Acoustic Library, Acoustic Toolbox, RAMSsurf. [accessed Fev. 07, 2016].

Oleson, E.M., Calambokidis, J., Burgess, W.C., McDonald, M.A., LeDuc, C.A., and Hildebrand, J.A. 2007. Behavioral context of call production by eastern North Pacific blue whales. Mar. Ecol. Prog. Ser. 330: 269-284.

Ramp, C., and Sears, R. 2012. Distribution, densities, and annual occurrence of individual blue whales (*Balaenoptera musculus*) in the Gulf of St. Lawrence, Canada from 1980-2008. DFO Can. Sci. Adv. Sec. Res. Doc. 2012/157. vii + 37.

Richardson, W.J., Greene, C.J., Malme, C., and Thomson, D. 1995. Marine mammals and noise. Academic Press, New York.

Ross, D. 1976. Mechanics of underwater noise. Pergamon Press, New York.

Sears, R., and Calambokidis, J. 2002. Update COSEWIC status report on the Blue Whale *Balaenoptera musculus* in Canada. COSEWIC assessment and update status report on the Blue Whale *Balaenoptera musculus* in Canada Committee on the Status of Endangered Wildlife in Canada., Ottawa.

Senneville, S., and Lefaivre, D. 2015. Reproduction horaire et à trois dimensions des conditions hydrographiques et hydrodynamiques du golfe du Saint-Laurent avec le modèle MoGSL pour la période de 1997 à 2014. *In* Rapport 2014-2015 de l'entente de contribution entre le MPO et l'ISMER/UQAR pour la simulation numérique des océans. *Edited by* M.L.I. Fisheries and Oceans Canada, Mont-Joli.

Simard, Y. 2009. Le Parc Marin Saguenay–Saint-Laurent: processus océanographiques à la base de ce site d'alimentation unique des baleines du Nord-Ouest Atlantique. The Saguenay–St. Lawrence Marine Park: oceanographic process at the basis of this unique forage site of Northwest Atlantic whales. Rev. Sc. Eau / J. Water Sci. 22(2): 177-197.

Simard, Y., Marcotte, D., and Naraghi, K. 2003. Three-dimensional acoustic mapping and simulation of krill distribution in the Saguenay - St. Lawrence Marine Park whale feeding ground. Aquat. Liv. Res. 16(3): 137-144.

Simard, Y., Lepage, R., and Gervaise, C. 2010. Anthropogenic sound exposure of marine mammals from seaways: Estimates for lower St. Lawrence Seaway, eastern Canada. Appl. Acoust. 71: 1093-1098.

Simard, Y., Roy, N., Giard, S., and Yayla, M. 2014. Canadian year-round shipping traffic atlas for 2013: Volume 1, East Coast marine waters. Can. Tech. Rep. Fish. Aquat. Sci. 3091(Vol.1) E: xviii + 327 pp

Simard, Y., Roy, N., Gervaise, C., and Giard, S. 2016a. Analysis and modeling of 255 ship source levels from an acoustic observatory along St. Lawrence Seaway J. Acoust. Soc. Am. 140(3): 000-000. (in press)

Simard, Y., Roy, N., Gervaise, C., and Giard, S. 2016b. A seaway acoustic observatory in action: The St. Lawrence Seaway. *In* The effects of noise on aquatic life II. *Edited by* A. Popper and T. Hawkins. Springer, New York. pp. 1031-1040.

Širović, A., Hildebrand, J.A., and Wiggins, S.M. 2007. Blue and fin whale call source levels and propagation range in the Southern Ocean. J. Acoust. Soc. Am. 122(2): 1208-1215.

Southall, B.L., Bowles, A.E., Ellison, W.T., Finneran, J.J., Gentry, R.L., Greene Jr, C.R., Kastak, D., Ketten, D.R., Miller, J.H., Nachtigall, P.E., Richardson, W.J., Thomas, J.A., and Tyack, P.L. 2007. Marine mammal noise exposure criteria: Initial scientific recommendations. Aquat. Mamm. 33(4): 410-522.

Sturm, F. 2005. Numerical study of broadband sound pulse propagation in three-dimensional oceanic waveguides. J. Acoust. Soc. Am. 117(3): 1058-1079.

Weilgart, L.S. 2007. The impacts of anthropogenic ocean noise on cetaceans and implications for management. Can. J. Zool. 85 (11): 1091-1116.

Wenz, G.M. 1962. Acoustic ambient noise in the ocean: Spectra and sources. J. Acoust. Soc. Am. 34(12): 1936-1956.

TABLES

Table 1. Mean and S.D. of risk estimate error (%) at the different frequencies and depths from the comparison of the simulated SPL and AS[4] in situ measurements, filtered (bold) and unfiltered (not bold) for pseudo-noise contamination.

Depth	Frequency			
	16 Hz	**20 Hz**	**40 Hz**	**63 Hz**
62 m	5.6 ± 12.1 **2.7 ± 5.7**	2.4 ± 5.9 **0.1 ± 3.4**	0.3 ± 1.9 **-0.1 ± 2.8**	0.9 ± 1.7 **0.4 ± 1.8**
161 m	5.0 ± 12.3 **2.3 ± 5.1**	2.2 ± 5.8 **-0.3 ± 3.58**	0.7 ± 2.9 **-0.4 ± 3.97**	0.6 ± 1.6 **0.5 ± 1.4**
288 m	4.5 ± 10.7 **1.6 ± 3.4**	1.2 ± 3.5 **-1.1 ± 4.8**	-0.1 ± 2.7 **-0.7 ± 4.1**	0.0 ± 2.8 **0.0 ± 2.8**

FIGURES

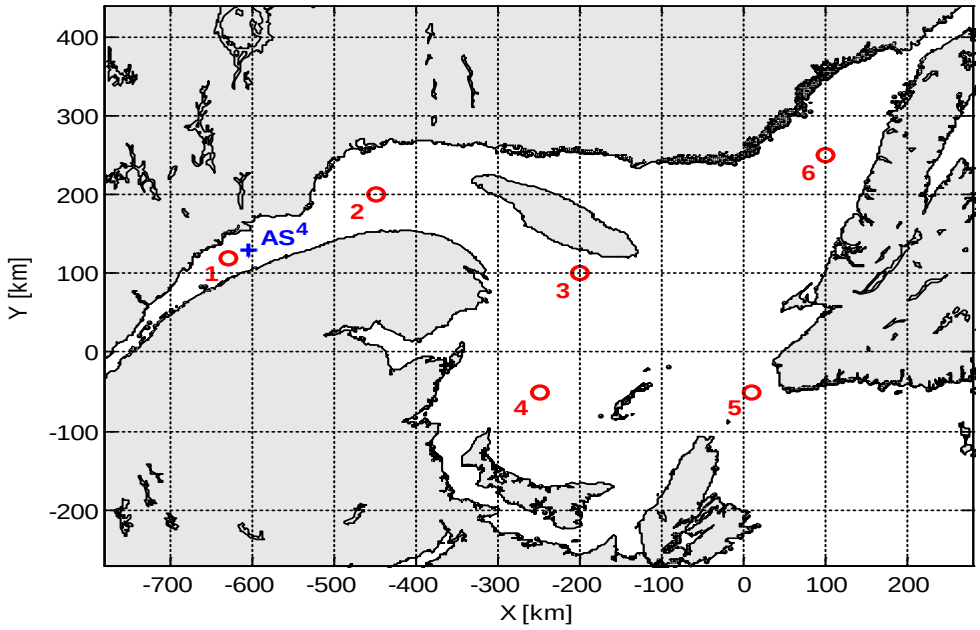

Figure 1. Map of the study area with locations of the AS^4 seaway acoustic observatory (+), and 6 representative points of interest (o) used in the text.

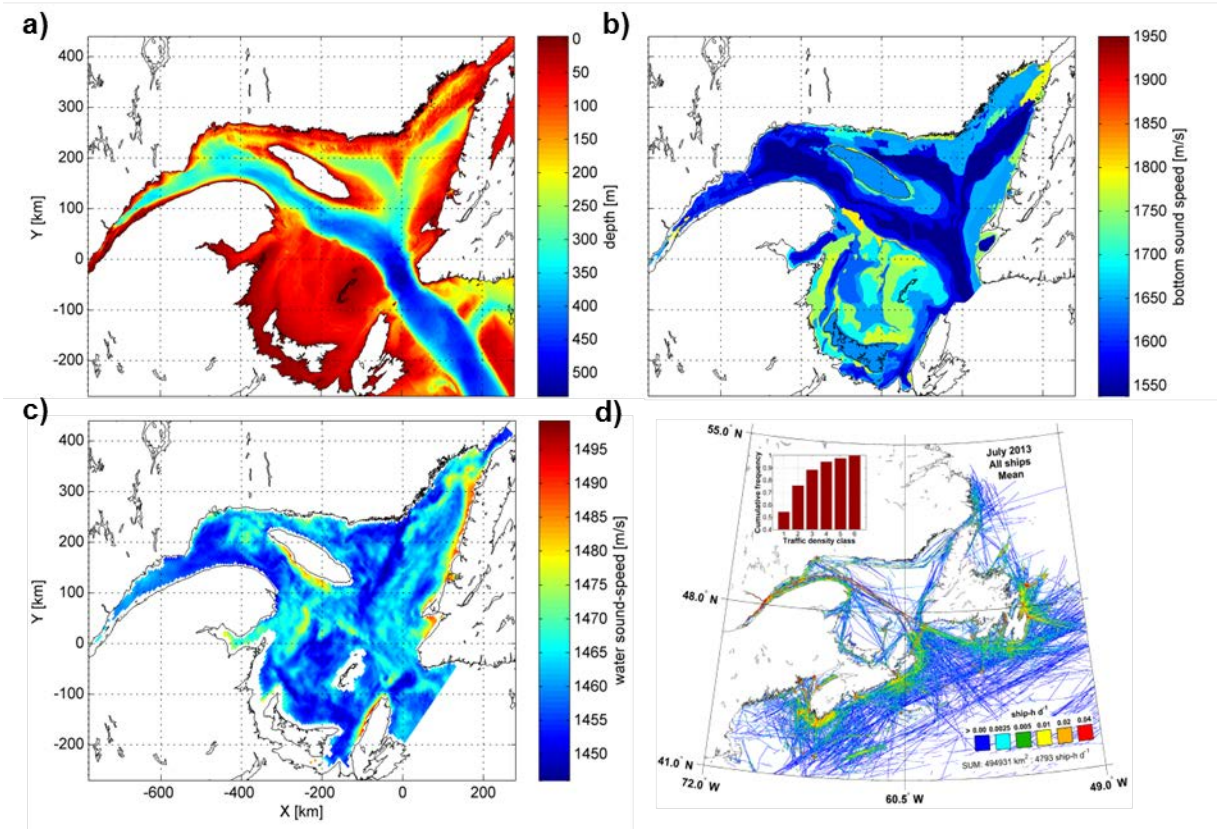

Figure 2. Example of inputs of the shipping noise simulation modeling. a) Bathymetry, b) Bottom sound speed, c) water sound speed at 25 m depth on July 1st 2013, 01:00 UTC, d) Mean AIS daily shipping traffic in July 2013.

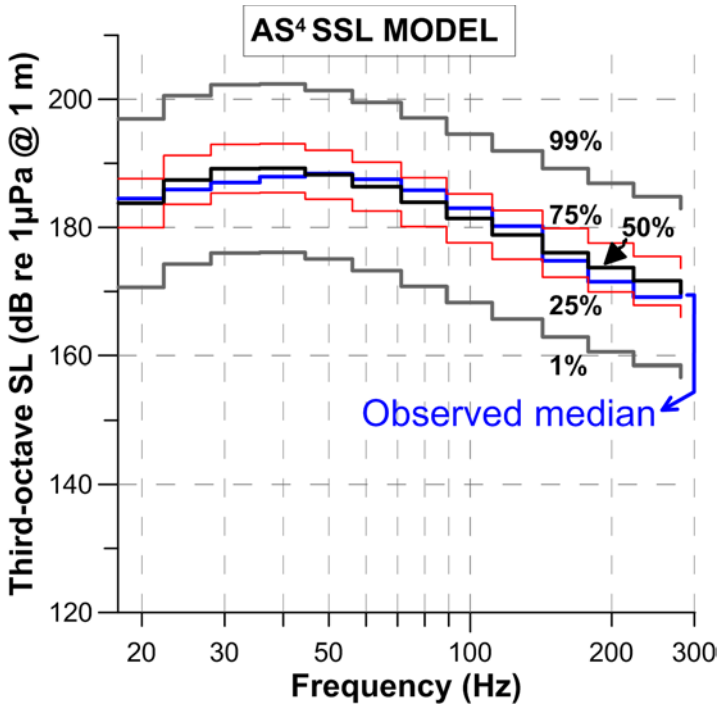

Figure 3. Ship source level statistics given by Simard et al. 2016.

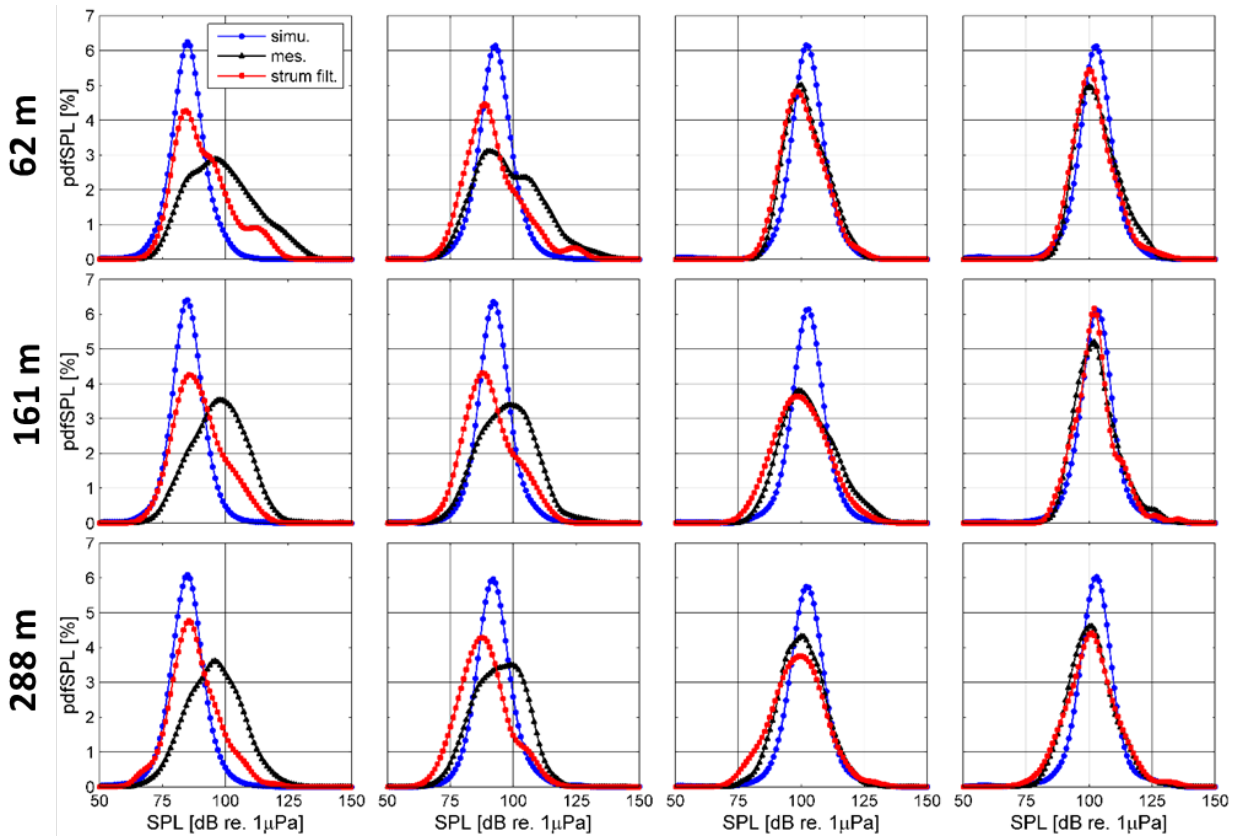

Figure 4. Simulated shipping noise pdfSPL (blue dotted line) are compared with AS[4] in situ measurements before (black triangle curve) and after exclusion of samples contaminated with pseudo-noise induced from mooring strumming, vibrations and flow around the hydrophone (red triangle line) for three depths: 62 m, 161 m and 288 m; and four one-third-octave band centered on 16 Hz, 20 Hz, 40 Hz and 63Hz.

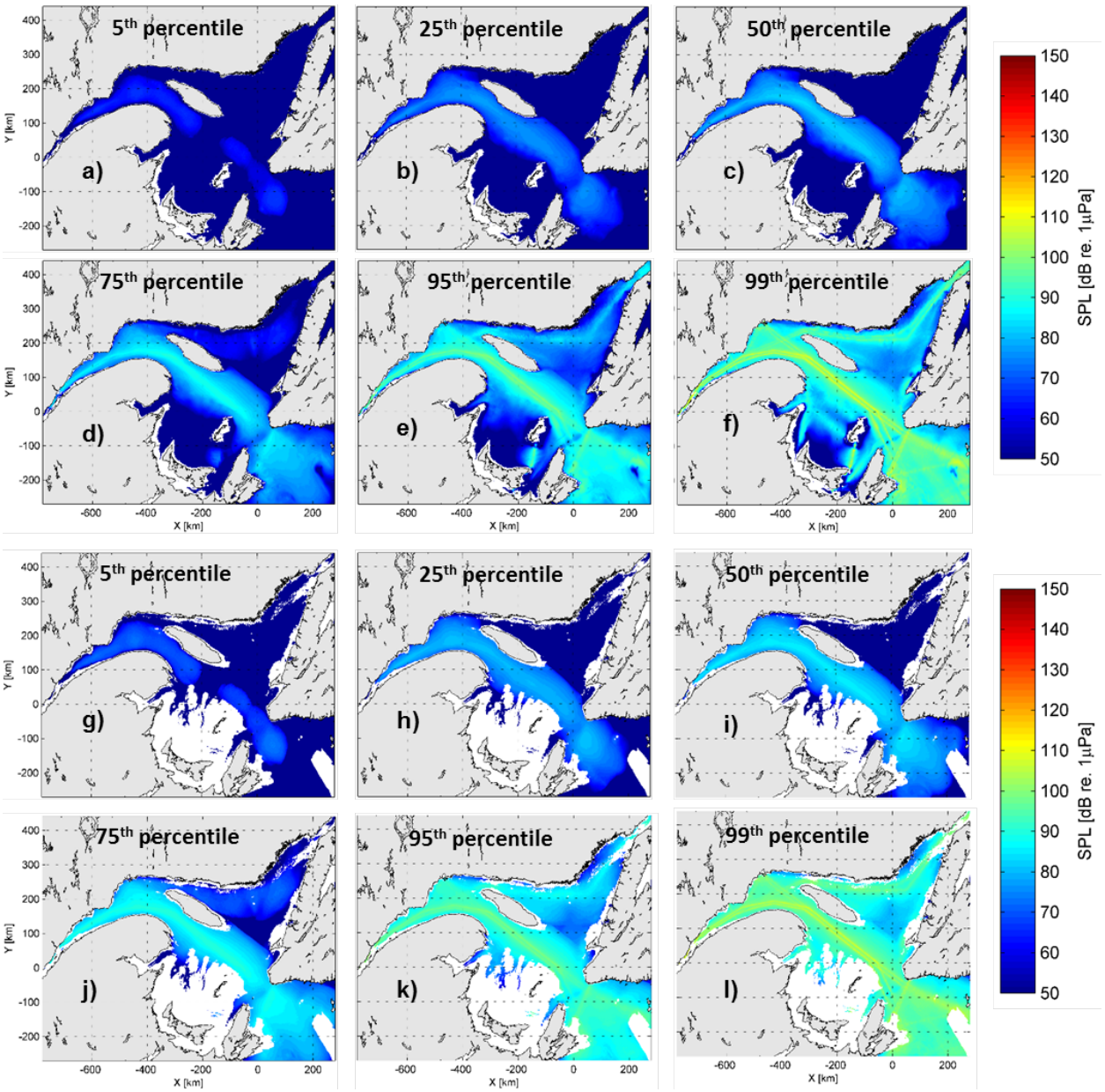

Figure 5. 16-Hz one-third-octave shipping noise level 5th, 25th, 50th, 75th, 95th and 99th centiles in July 2013 at depths of: 25 m a), b), c), d), e) and f) and 75 m g), h), i), j), k)and l).

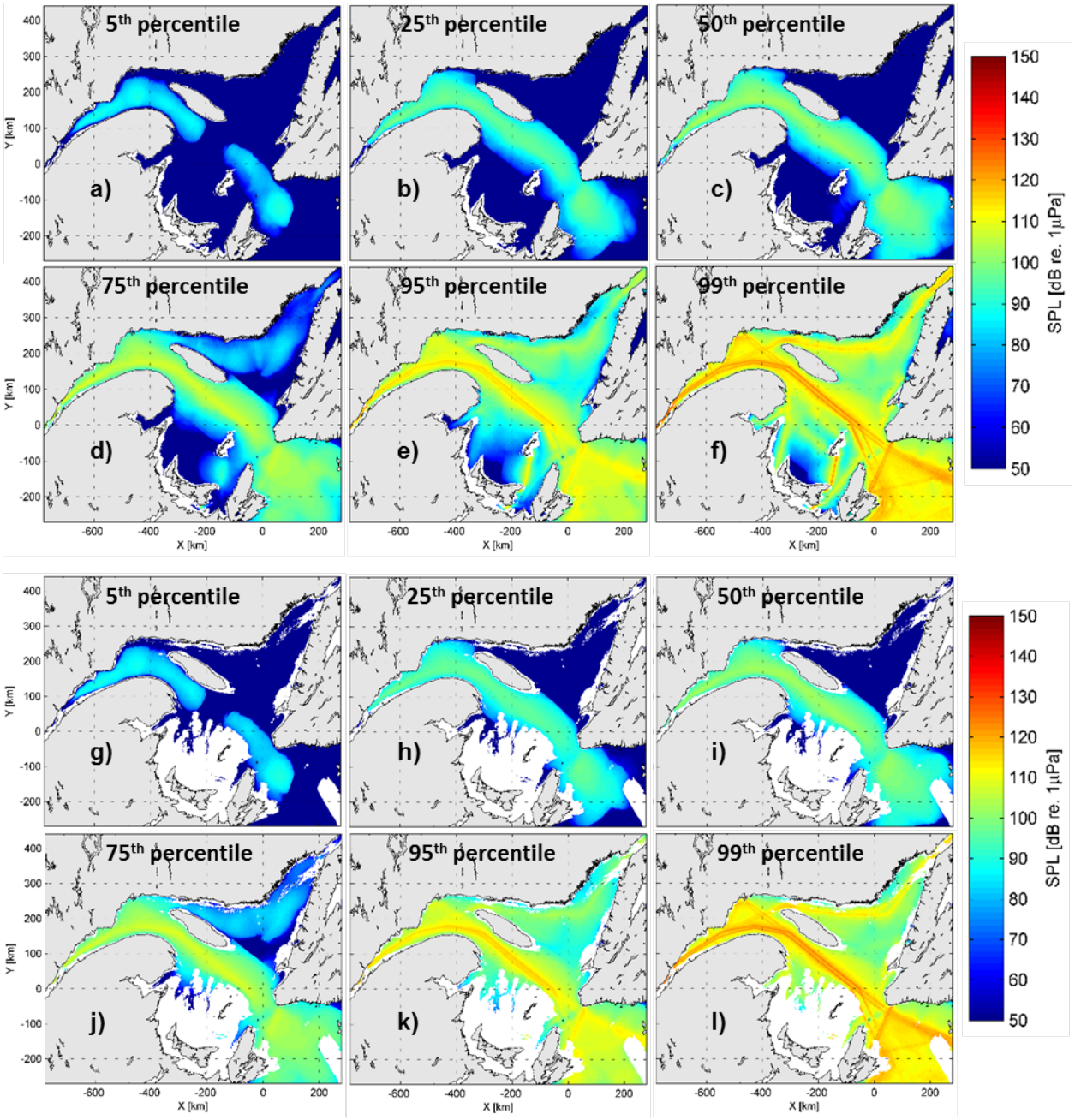

Figure 6. 63-Hz one-third-octave shipping noise level 5th, 25th, 50th, 75th, 95th and 99th centiles in July 2013 at depths of: 25 m a), b), c), d), e) and f) and 75 m g), h), i), j), k)and l).

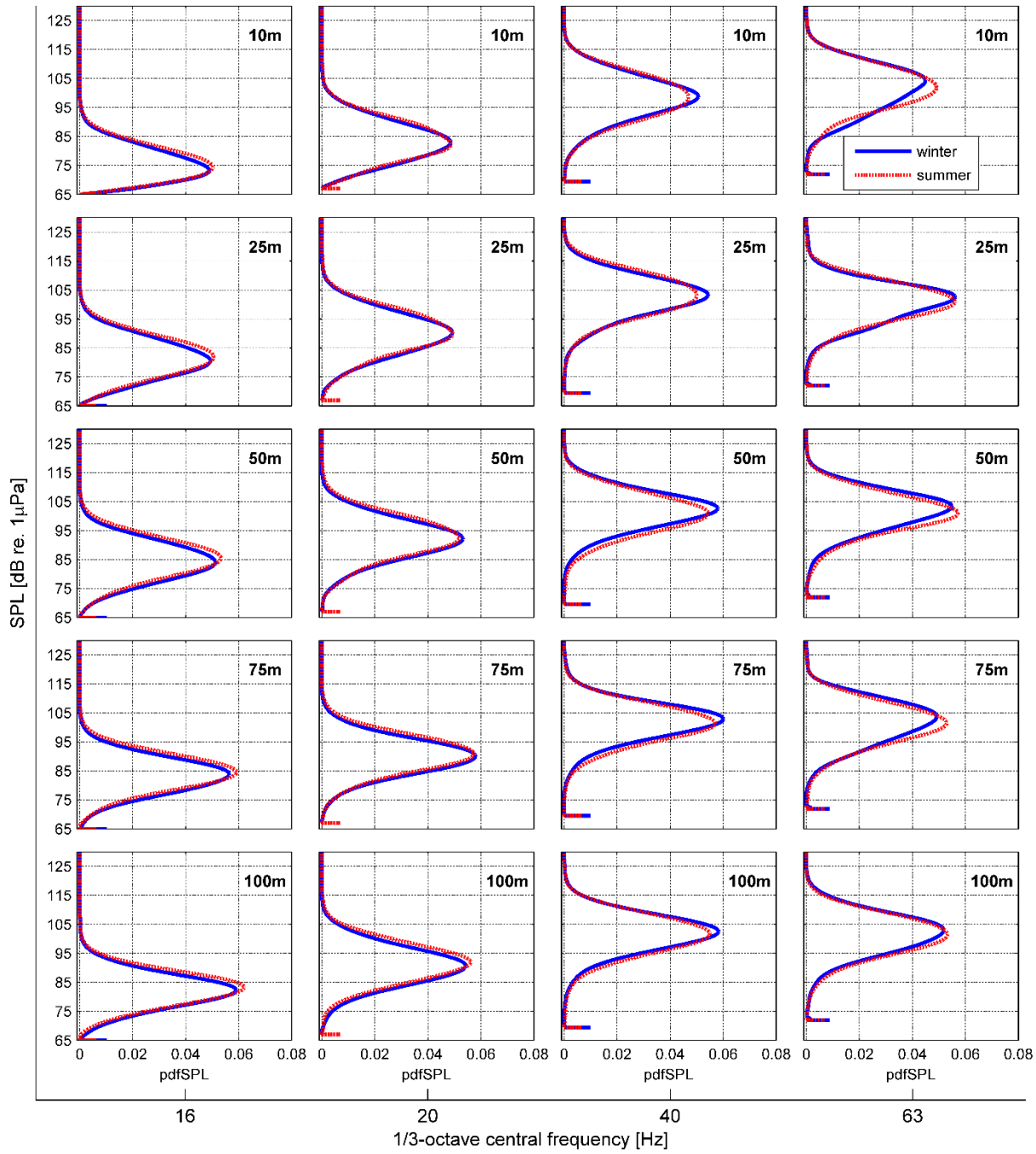

Figure 7. Pdfs of shipping and ambient noise SPL at 16, 20, 40, and 63 Hz one-third-octave bands for 10, 25, 50, 75 and 100 m depths at location 3 (Fig. 1). The reference lowest ambient noise levels (ANL) are, for each frequency respectively, 65, 67, 69.5, and 72 dB re 1 µPa (Gervaise et al. 2012).

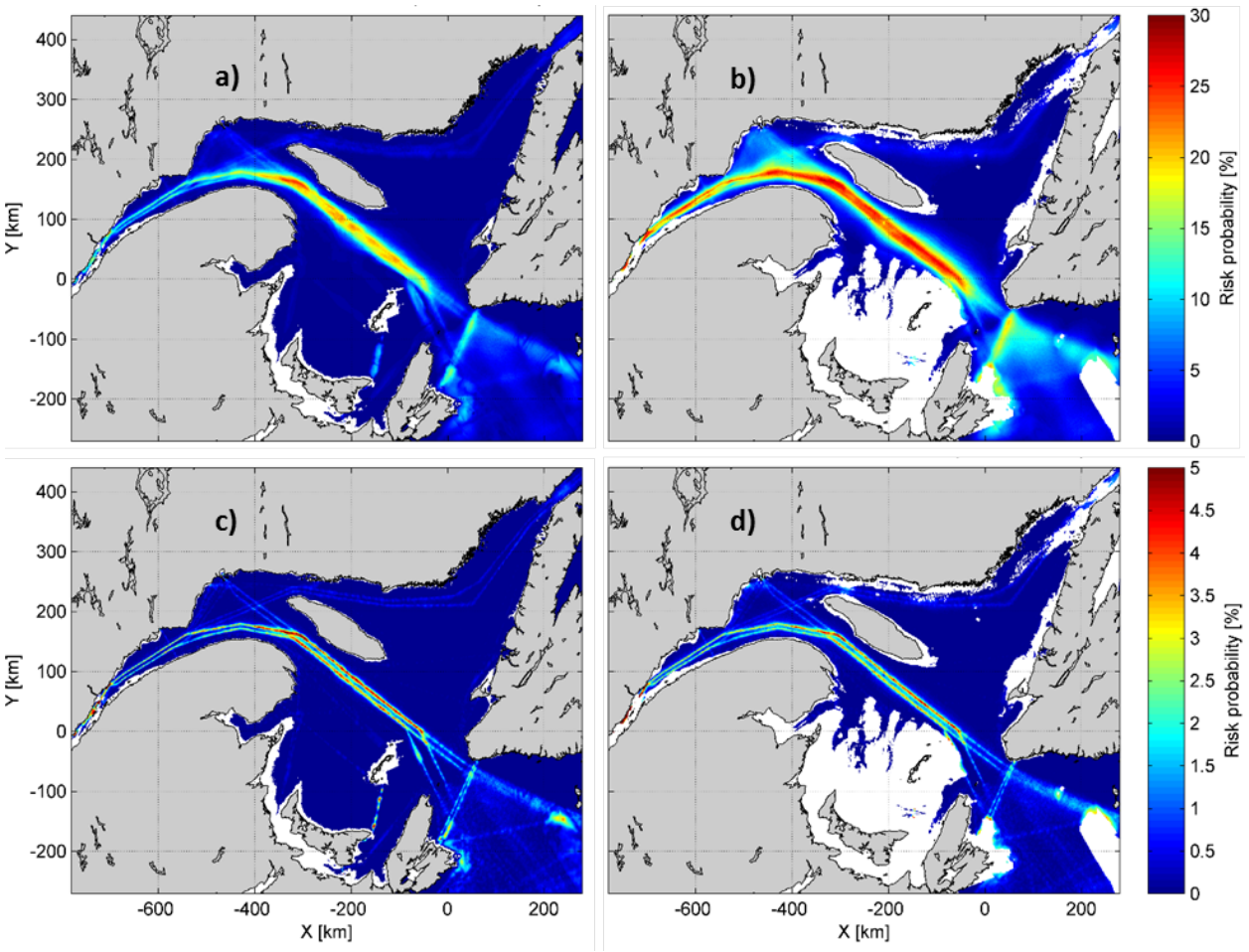

Figure 8. Risk that 16-Hz one-third-octave shipping noise SPL in July 2013 is higher than: 90 dB re 1 µPa at 25 (a) or 75 m depths (b), and 100 dB re 1 µPa at 25 (c) or 75 m depths (d). Note the colorbar change between the top and bottom panels.

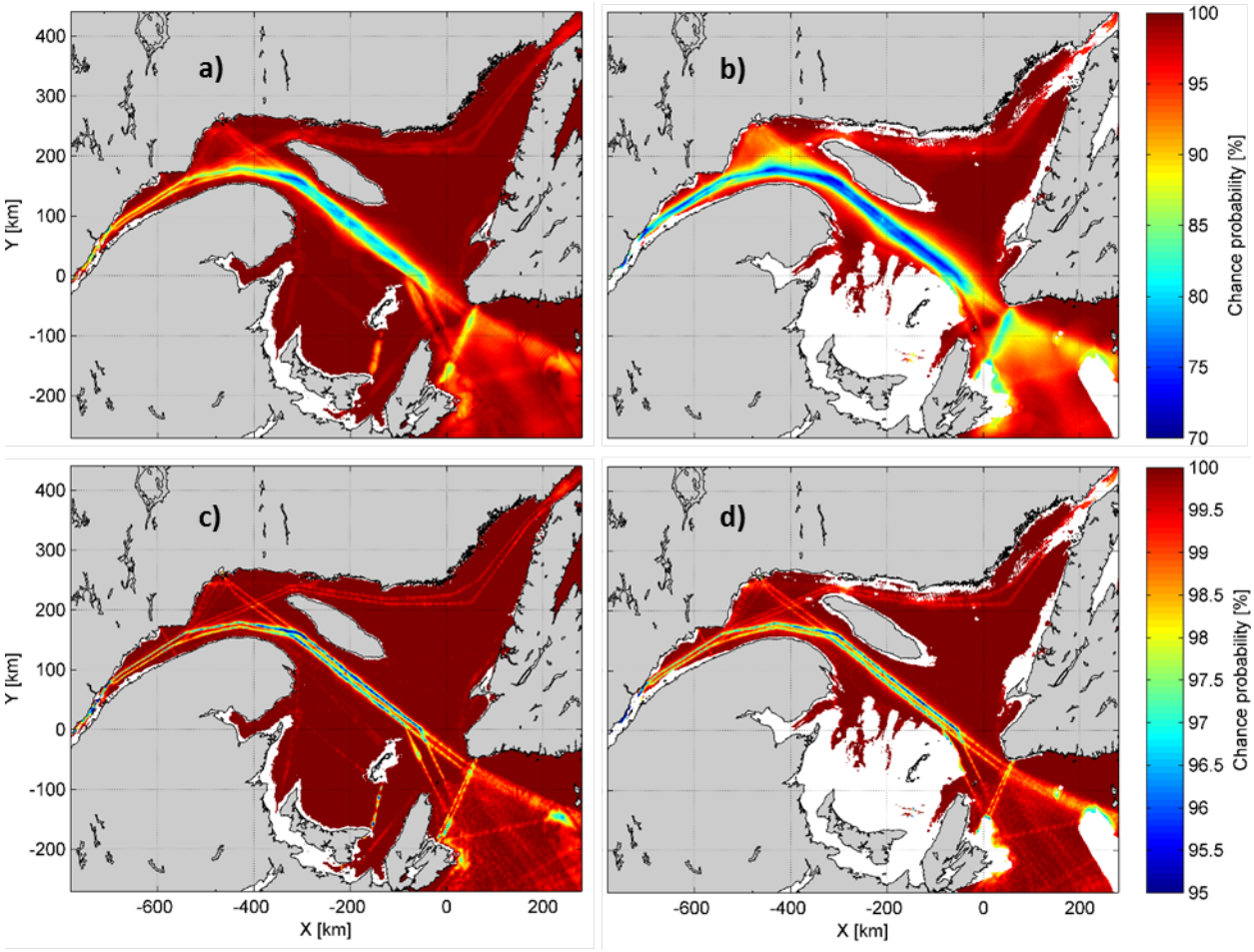

Figure 9. Chance that 16-Hz one-third-octave shipping noise SPL in July 2013 is lower than: 90 dB re 1µPa at 25 a) or 75 m depths b), and 100 dB re 1µPa at 25 c) or 75 m depths d). Note the colorbar change between the top and bottom panels.

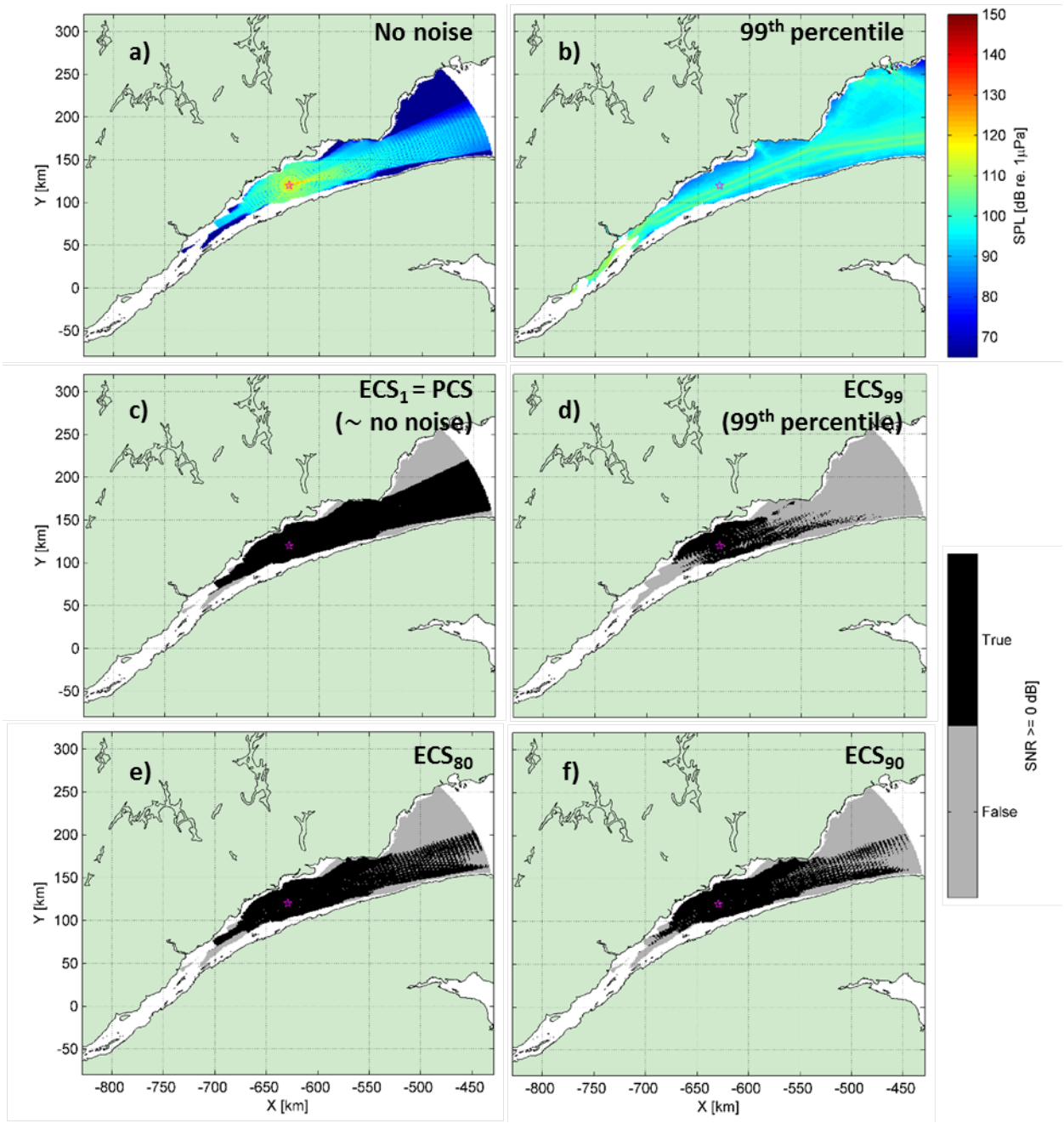

Figure 10. Blue whale A-call sender ECS_i in Lower Estuary. a) received levels at a depth of 50 m from a 15-m 190-dB re 1 µPa @ 1 m emission of a 16-Hz one-third-octave A-call at point of interest 1 (Fig. 1) on July 1st, 2013; b) 99th centile of 16-Hz one-third-octave shipping noise SPL in July 2013; c) sender ECS_1 corresponding to the lowest 1% of July shipping noise SPL (i.e. PCS), d) ECS_{99} corresponding to the highest 1% of July shipping noise SPL , e) the highest 20% of July shipping noise SPL (ECS_{80}), and f) the highest 10 % of July shipping noise SPL (ECS_{90}).

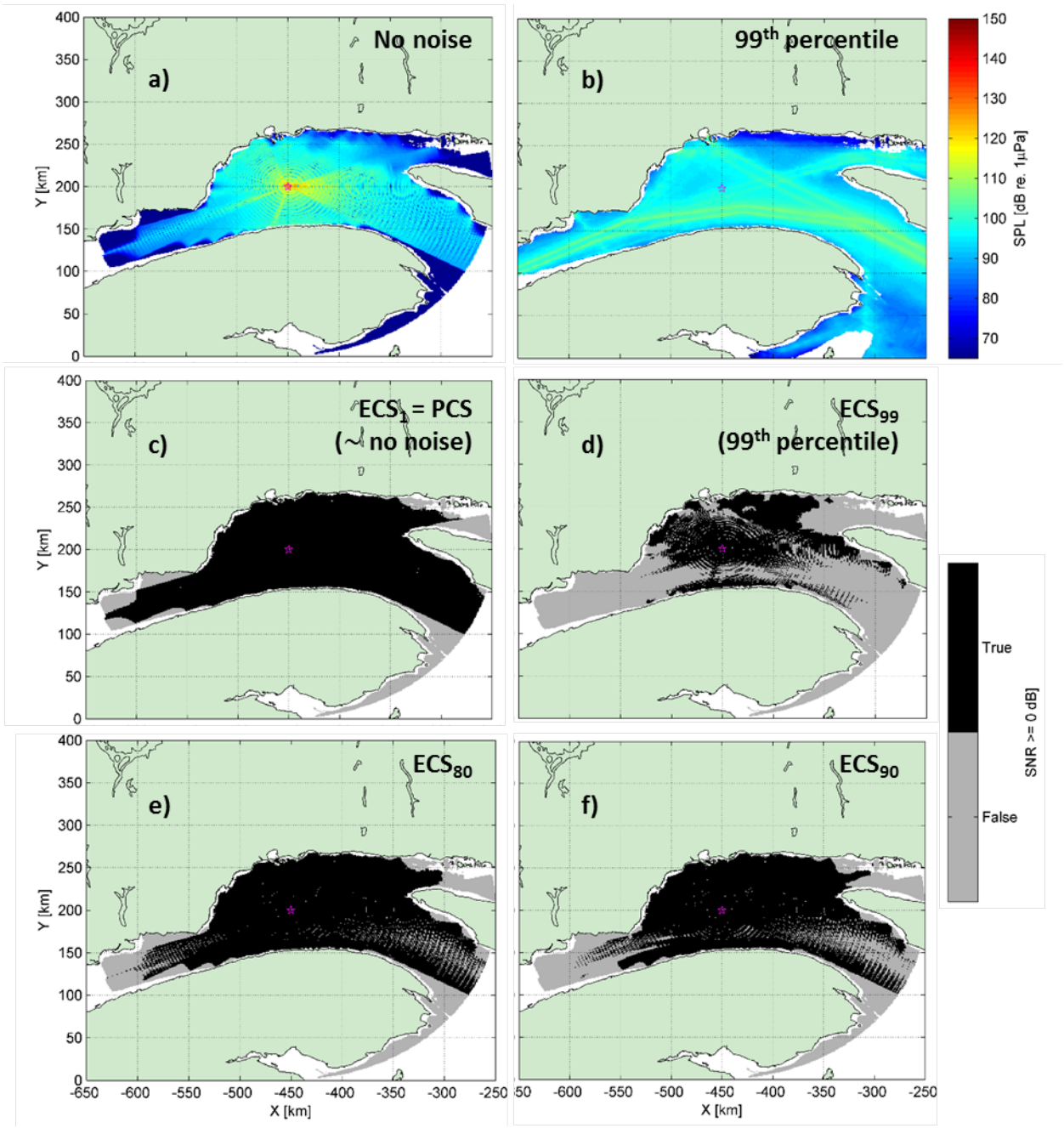

Figure 11. Blue whale A-call sender ECS_i in Northwest Gulf of St. Lawrence point of interest 2 (Fig. 1). Legend as in Fig. 10

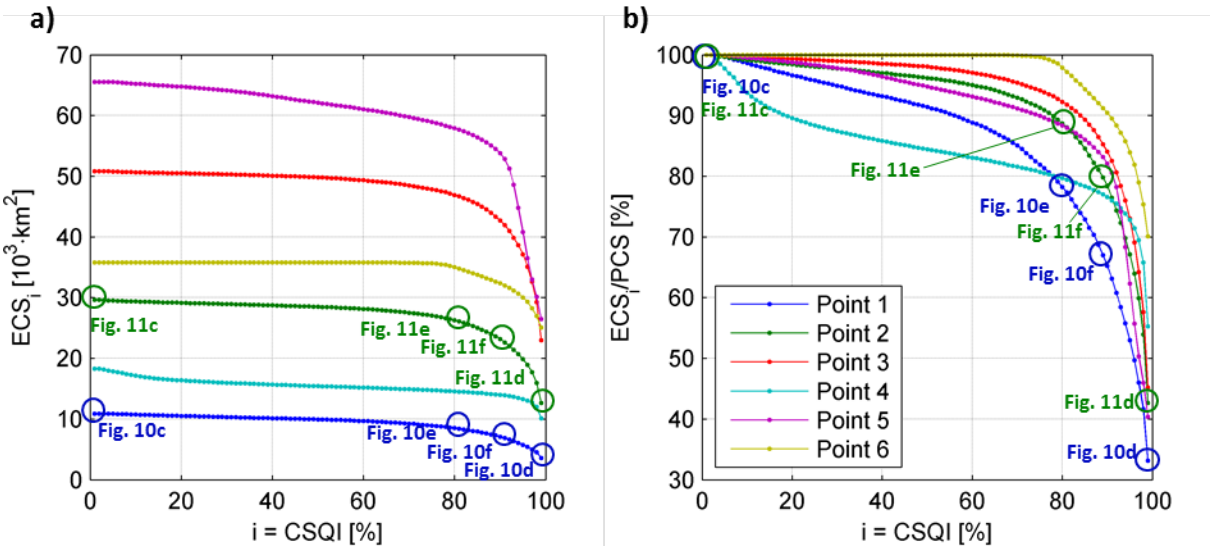

Figure 12. A-call sender ECS$_i$ at 50 m as a function of CSQI values, i, for a 15-m 190-dB re 1 µPa @ 1m calling blue whale at points of interest 1 to 6 (Fig. 1) i.e. sum of the area where communication is possible at least i% of the time: a) absolute areas, b) relative to the local PCS at the corresponding point.

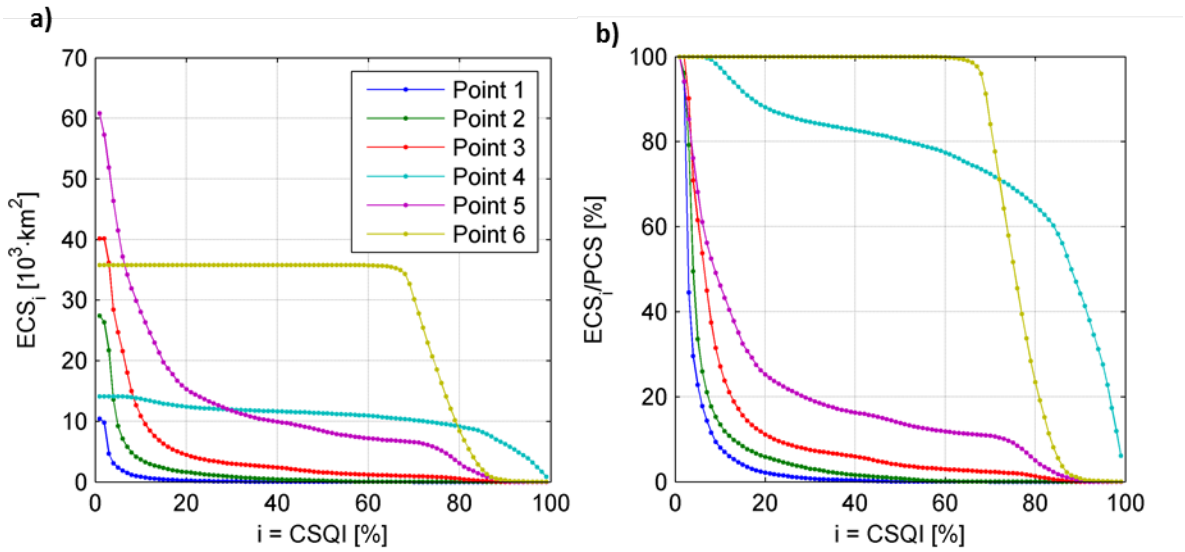

Figure 13. D-call sender ECS$_i$ as a function of CSQI values, i, for a 15-m 160-dB re 1 µPa @ 1 m calling blue whale for points of interests 1 to 6 (Fig. 1) i.e. sum of the area where communication is possible at least i% of the time: a) absolute areas, b) relative to the local PCS at the corresponding point.